JOURNAL OF MATERIALS SCIENCE 26 (1991) 1677–1682

Undercooling and formation of bulk metallic glass of Pd–Ni–P in a containerless environment

YINGFAN XU, WENKUI WANG
Institute of Physics, Academia Sinica, PO Box 603, Beijing 100080, People's Republic of China

Undercooling experiments on $Pd_{40}Ni_{40}P_{20}$ alloy were performed in a laboratory-scale drop tube. The effect of cooling rates on nucleation and crystal growth of the alloy was studied by changing the inert gases in the tube and the critical cooling rate for glass formation in the tube was determined. In addition, the results indicate that the superheat of the drop before it dropped down is closely related to nucleation and crystal growth of the alloy.

1. Introduction

Heterogeneous nucleation occurs mainly on the crucible's wall and impurities in melt or surface oxides when the melt is cooled from above its melting temperature. To avoid crystal nucleation and growth, a cooling rate in a range of 10^4 to 10^7 K/s is generally needed. However, if the containerless technique is used, heterogeneous nucleation occurring on the wall could be eliminated and a lower cooling rate for the glass formation is permitted [1–3]. In the case of $Pd_{40}Ni_{40}P_{20}$, it is reported that glass spheres of up to 1 mm diameter had been formed in a 3 m drop tube [4]. In the present work we have studied the undercooling and nucleation of the $Pd_{40}Ni_{40}P_{20}$ melt solidified in a 1.2 m drop tube and the effect of cooling rates on the melt solidification process by changing the gases in the drop tube.

The tube was evacuated to 1.33×10^{-3} Pa and then filled with pure helium and argon, respectively, so that different heat extraction conditions could be reached. By analysing the dropped samples carefully, the process of glass formation, crystal nucleation and growth in the undercooled $Pd_{40}Ni_{40}P_{20}$ melt was observed.

2. Experimental procedure

The $Pd_{40}Ni_{40}P_{20}$ alloy ingots were prepared by arc melting the mixture of pure Pd (99.9 wt %) with Ni_2P which was alloyed by sintering pure Ni (99.6 wt %) with pure P (99.3 wt %) at a temperature of 1100 K for two days. The analytic composition of the alloy deviated slightly from the nominal values.

Spherical drops were prepared by dispersing the molten alloy from a quartz nozzle at the top of the drop tube. The tube was evacuated to 1.33×10^{-3} Pa and filled with pure helium or argon gas, then evacuated and refilled a second time. After refilling a third time, the tube was ready to use. A molybdenum resistance heater was used to heat the nozzle and alloy to approximately 1050 K and 1250 K, respectively, well above the melting temperature of the alloy (885 K). When the alloy was melted, the higher pressure gas than in the tube was backfilled and this dispersed the melt into the tube with the creation of many drops. Samples under the following three environments were made: (a) in vacuum condition (1.33×10^{-3} Pa); (b) filled with helium at pressures of 79,800 Pa and 26,666 Pa; (c) filled with argon at pressures of 79,800 Pa and 26,666 Pa. The solidified samples were collected in the silicone oil at the bottom of the tube. The sizes of the drops ranged from 0.1 to 2.0 mm; the quartz nozzles had various orifice sizes within the range 0.1–0.6 mm.

The drops were identified by an X-ray position-sensitive proportional counter (PSPC) microdiffractometer, a differential thermal analyser (DTA), a scanning electron microscope (SEM), etc. The sphericity and smoothness of the drops were examined by SEM and an optical microscope. The samples for metallograph were etched in dilute aqua regia for 3 to 5 minutes at room temperature.

3. Results

Fig. 1a shows the shape and surface appearance of $Pd_{40}Ni_{40}P_{20}$ glassy droplets caught at the bottom of the drop tube. All the drops showed a smooth surface and spherical shape except the one at the bottom left. Fig. 1b is a micrograph showing the shape and cross-sectional structure of a glassy sphere with a diameter of 1.6 mm. The results for the spheres solidified in various gases and in vacuum at initial temperature of 1050 K are summarized in Table I.

From Table I we can see that the spheres solidified in 79,800 Pa helium gas are composed of a single glass phase with diameter in a range from approximately 0.1 to 1.8 mm, while some spheres larger than about 1.3 mm in diameter solidified in 26,666 Pa helium gas show some initial phase in the glass matrix (Fig. 2). Their shapes are trefoil and quatrefoil-like (Fig. 2b) and their size is about 3 μm. These phases cannot be detected by the X-ray PSPC microdiffractometer because their volume fraction is less than 5%. The average composition of these initial phases revealed by an electron probe is $Pd_{36.2}Ni_{51.4}P_{12.4}$, different from

0022–2461/91 $03.00 + .12

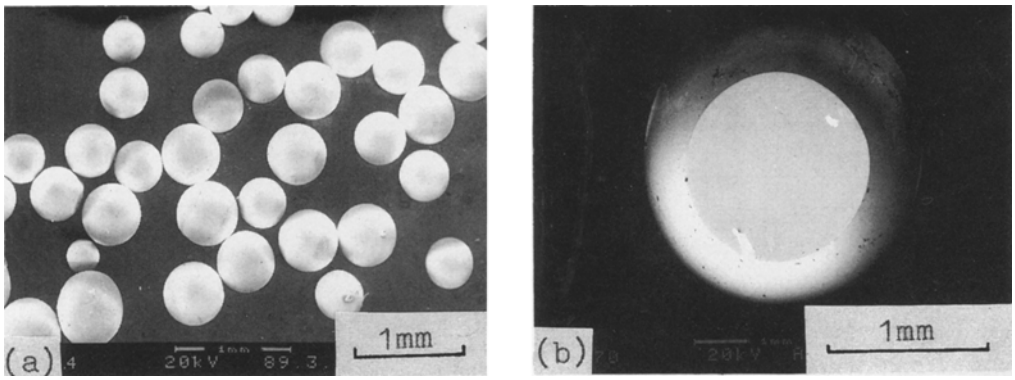

Figure 1 Scanning electron micrograph of the $Pd_{40}Ni_{40}P_{20}$ drops: (a) a collection of $Pd_{40}Ni_{40}P_{20}$ glassy spheres; (b) the shape and cross-sectional structure of a sphere with a diameter of 1.6 mm.

TABLE I Summary of the results of $Pd_{40}Ni_{40}P_{20}$ spheres solidified in three environments, initial temperature is 1050 K

Diameter range (mm)	He (Pa)		Ar (Pa)		Vacuum (Pa)
	79,800	26,666	79,800	26,666	1.33×10^{-3}
0.1–0.6	G	G	G	G	G + C
0.7–1.2	G	G	G + D	G + D	G + C
1.3–1.8	G	G + D	G + D	G + D	G + C, C

Key: G means glass phase, D means initial phase and dendrites, C means spherical crystals.

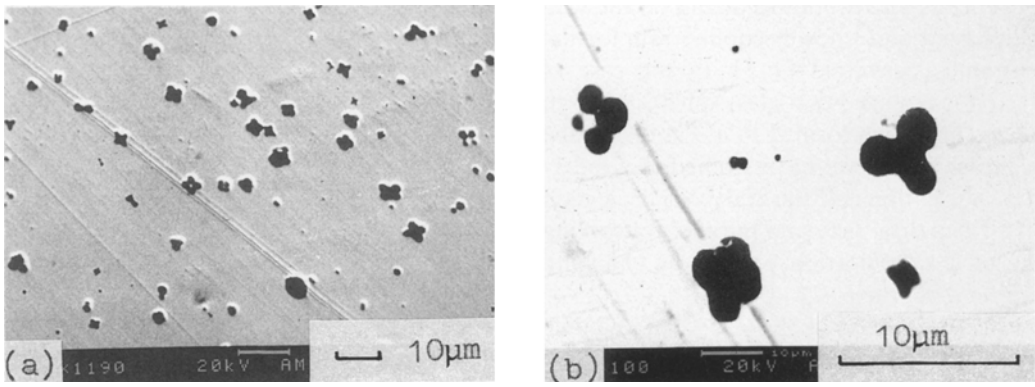

Figure 2 Microstructure of a sphere (in 26,666 Pa He) with a diameter of 1.8 mm: (a) many primary trefoil and quatrefoil-like phases appeared in the glass matrix; (b) a magnified view.

that of the glass matrix of $Pd_{38.0}Ni_{44.1}P_{17.9}$. The estimated measurement error is about $\pm$ 3 at %.

As the initial melt temperature increased to about 1250 K, the number of primary phases reduced greatly and almost none of them was observable. However, when the temperature further increased, some drops did not solidify as spheres but in elliptical or irregular shapes owing to the melt touching the bottom of the tube (Fig. 3).

The spheres solidified in argon gas with diameters of about 0.1 to 0.6 mm are single glass phase, while those with diameter larger than 0.6 mm are composed of glass plus the small dendrites. The dendrites grew along tetragonal and triangular directions, with crosswise about 10 μm, as shown in Fig. 4. Also the diffractions of these dendrites could not be found by the X-ray PSPC microdiffractometer and the spectrum showed only the glass pattern. Electron probe analysis revealed that the composition at the centre of the dendrites is similar to that of the primary phase, and that at the trunk of a dendrite it is $Pd_{41.3}Ni_{40.5}P_{18.2}$, close to that of the glass matrix. Their positions are noted as a, b and c, respectively, in Fig. 4a.

In the case of the vacuum environment, spheres with diameter ranging from about 0.1 to 1.5 mm are composed of the glass phase plus spherical crystals (see Fig. 5). Carefully analysing Fig. 5b, it can be seen that the trefoil and quatrefoil dendrites also appeared at the centre of the spherical crystals, and some small trefoil and quatrefoil patterns, like those shown in Fig. 2, also appeared in the glass matrix. The lamellae structure grew on the dendrites radially. The overall composition of the lamellar structure is similar to that of the glass phase, and the composition of the centre of the dendrites is similar to that of the primary phase. The X-ray diffraction pattern shows that the sharp crystallized peaks overlapped the broad glass peak indicating the partial crystallization (Fig. 6b). The

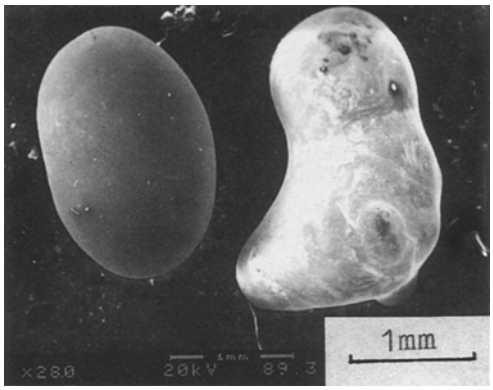

Figure 3 Samples solidified in ellipsoidal and irregular shapes as the T_i of the melt was too high.

scribed by a differential equation as [5]

$$dT/dt = (-\varepsilon\sigma(T^4 - T_0^4) - h(T - T_0))(6/C_p\rho d) \quad (1)$$

where T is the drop temperature, ε is the emittance, σ is the Stefan–Boltzman constant, h is the heat transfer coefficient, C_p is the heat capacity and ρ is the density of the alloy. In using Equation 1 it is assumed that there are no temperature gradients within the drop, that no phase change occurs, and that the temperature of the gas far from the drop and the environment temperature are both T_0.

An iteration method applied to Equation 1 was used to calculate the temperature of a liquid droplet as

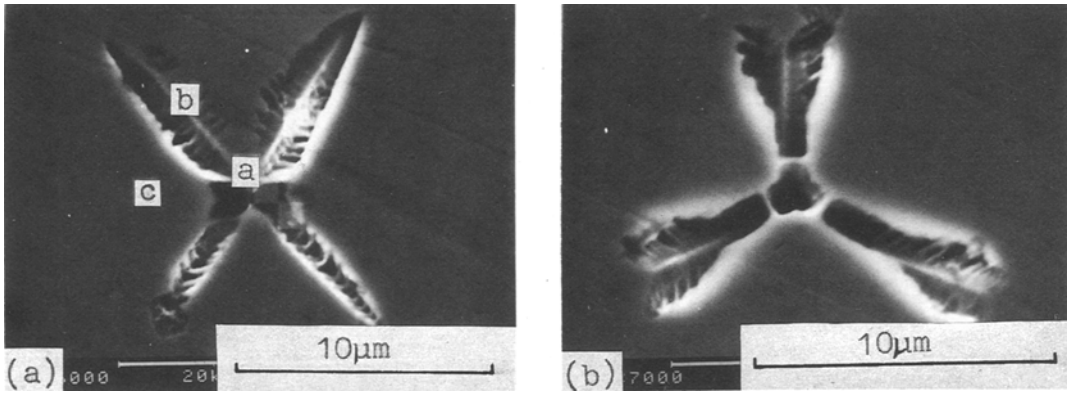

Figure 4 Microstructure of a sphere (in 26,666 Pa Ar) with a diameter of 1.9 mm, containing dendrites in the glass matrix: (a) quatrefoil dendrites, with a: the centre, b: the trunk, and c: the glass matrix; (b) trefoil dendrites.

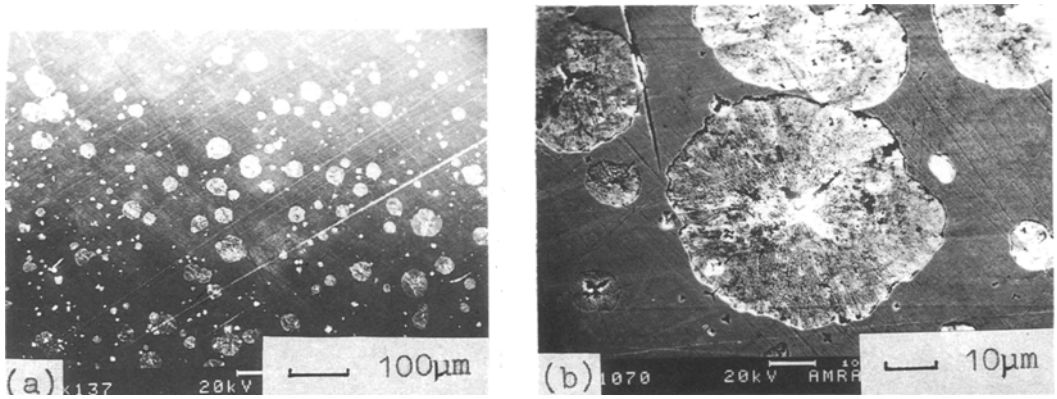

Figure 5 Microstructure of a sphere (in vacuum) with a diameter of 1.45 mm: (a) some spherical crystals in the glass matrix; (b) a magnified view.

spheres with diameter larger than 1.5 mm are completely crystallized (Fig. 6c), showing eutectic solidification.

4. Heat flow analysis

To understand the cooling behaviour of $Pd_{40}Ni_{40}P_{20}$ drops further, the cooling rates of the drops in the tube were calculated. In the tube a liquid droplet cooled down partly by radiative heat transfer but mostly by convective heat transfer. The temperature history of a liquid droplet in drop tube processing can be described as a function of fall time in the drop tube. The results indicated that with increasing d, the diameter of the sphere, a longer falling time is required to reach the same undercooling. Also, because the heat extraction rate is decreased, a longer falling time is required for the same size drop in argon gas than in helium, indicating the decreased cooling rate. Fig. 7 shows the cooling rate of drops with various diameters in helium and argon gas at a temperature of T_g (590 K). Compared with the results summarized in Table I, the critical cooling rate for glass formation in drop tube processing was estimated. By eliminating wall hetero-

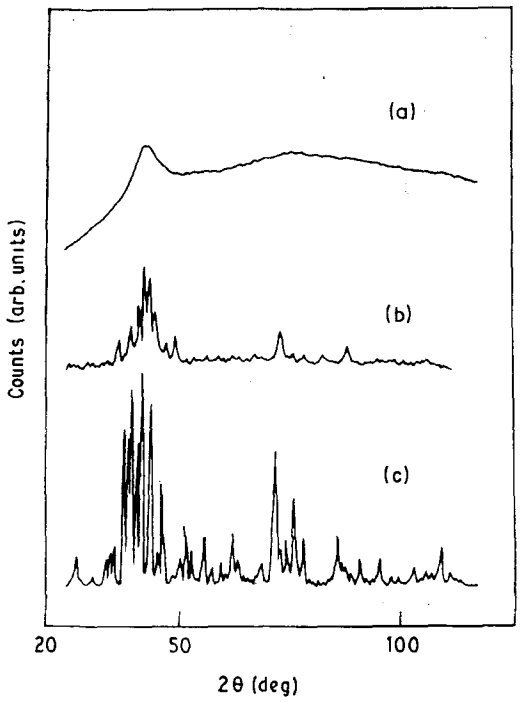

Figure 6 X-ray diffraction patterns: (a) spectrum of the glass spheres; (b) glass phase with some spherical-like crystals; (c) completely crystallized sphere.

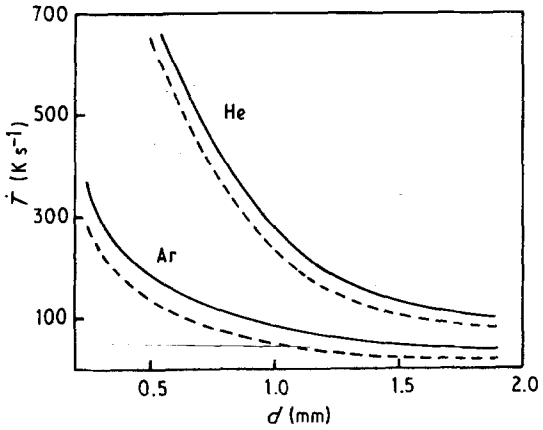

Figure 7 The calculated cooling rate (at 590 K) versus the drop diameter in He and Ar gas under pressures of 79,800 Pa (solid line) and 26,666 Pa (dashed line).

geneous nucleations, a cooling rate of 150 K/s was needed to avoid the drop interior nucleation.

5. Discussions

The free fall time provided by a 1.2 m drop tube is about 0.5 second. In the case of the vacuum environment, the melt drops are hardly solidified in such a short time solely by radiative thermal transport. As the tube is filled with inert gas, the thermal transport in the drops is combined with convection and radiation, and the convective term is much larger than the radiative term [3]. In our experiment, inert helium and argon gas were used. The thermal conductivity of helium is about one order of magnitude larger than that of argon gas [6], so the heat transfer coefficient of the droplet in helium gas is several times (approximately five times by our calculations) of that in argon gas. Therefore, by filling with various inert gases at various pressures in the tube, the thermal conditions of the molten drops are varied over a wide range. As a result, the different solidification morphologies of the drops were observed, allowing an insight into the crystal nucleation and growth process.

Fig. 7 shows the cooling rate, effected by the gas pressures, varying with the diameters of the drops. For diameters d smaller than about 1.0 mm, the cooling rate $\dot{T}$ decreased rapidly with the increasing of d; while for d larger than 1.0 mm, the $\dot{T}$ decreased slowly. This can be interpreted by the change of the heat transfer coefficient h according to Equation 1. h varies with the temperature, velocity and the diameter of the droplet, and can be described in terms of Nusselt number [5] through the equations

$$h = \mathrm{Nu} \times K_t/d \qquad (2)$$

$$\mathrm{Nu} = 2 + 0.3P_r \times \mathrm{Re}^{0.6} \qquad (\mathrm{Re} < 10^5) \qquad (3)$$

where K_t is the thermal conductivity of the gas, $P_r = C_p \times \eta_g/K_t$ is the Prandtl number, $\mathrm{Re} = \rho_g V_m d/\eta_g$ is the Reynolds number, C_p, η_g and ρ_g are the specific heat, viscosity and density of the gas, respectively, and V_m is the velocity of the drop. In this case the gas properties are evaluated at the film temperature $T_f = (T + T_0)/2$.

From Equations 1–3 we can see that the radiative term is proportional to d^{-1}, and the convective term is proportional to d^{-2}. Thus, with the increasing of d, h decreased with d, and the cooling rate $\dot{T}$ decreased with d^2 mainly, resulting in the change of solidification morphologies. In the previous work reported by Drehman *et al.* [4], since the drop tube was filled with helium at one atmosphere and the drop diameters were smaller than 1.0 mm, only the single glass phase of $Pd_{40}Ni_{40}P_{20}$ droplets was obtained by the drop tube process.

Davies has estimated that a critical cooling rate of 120 K/s was needed for the glass formation of $Pd_{40}Ni_{40}P_{20}$ alloy by using the classical homogeneous nucleation theory [7]. This value is in agreement with our result, estimated as 150 K/s. However, Drehman *et al.* had prepared the bulk $Pd_{40}Ni_{40}P_{20}$ glass with a cooling rate as low as 1 K/s [8], and found that the homogeneous nucleation rate is about $10^6/m^3s$ at a temperature of 590 K [4]. This value can produce the quenched-in nuclei density of $6 \times 10^4/m^3$, much smaller than our result of $1.4 \times 10^{13}/m^3$, estimated from Fig. 5a. This great discrepancy indicated that it is unlikely that the nucleation process occurring in our samples is homogeneous; more likely, it is heterogeneous. On the other hand, the homogeneous nucleation, an intrinsic process, can only be avoided by a cooling rate which is determined by the homogeneous nucleation rate; while the heterogeneous nucleation process can, in principle, be reduced by eliminating the heterogeneities. Therefore, it is possible to produce $Pd_{40}Ni_{40}P_{20}$ glass at a cooling rate lower than 1 K/s if heterogeneous nucleation is completely avoided. The cooling rate of 150 K/s is used to avoid interior heterogeneous nucleation in the drop tube process. The inadequate

value of 120 K/s, estimated by Davies, may be mostly due to the uncertainty of the thermal physical parameters such as viscosity, interfacial energy and Gibbs free energy, etc., which are difficult to determine by experiment.

The purity of the initial materials that we used is very low, so this may be a significant source of the much higher nucleus density in our samples. This has been supported by our results from electron probe microanalysis of the composition at the centre of the dendrites or the inclusions (Figs 2 and 4). The elements Al, Si and Mn appeared clearly in the X-ray energy spectrum (Fig. 8), and their contents were much higher than that at other places, such as at the trunk of the dendrites or the glass matrix. These inclusion elements may be present as oxides or compounds, and they can act as the nucleation centre during the cooling of the melt. As the initial temperature T_i of the drops increased, the Si content was absent and the Mg content reduced significantly, while the Al content was still present (see Fig. 9). This means that some Si and Mg compounds were dissolved or reduced. Since the melting temperature of Al is 933 K, the Al element appearing in the spectrum suggests that it may present as oxides. The melting temperature of the Al oxides is much higher than that of the element, so the Al oxides could not be dissolved by increasing the temperature in our experiment. This needs to be investigated further. Nevertheless, by increasing T_i, the inclusions compounds or oxides were partly dissolved or reduced, so that the nucleation events reduced significantly during the cooling of the drops. Thus the effect

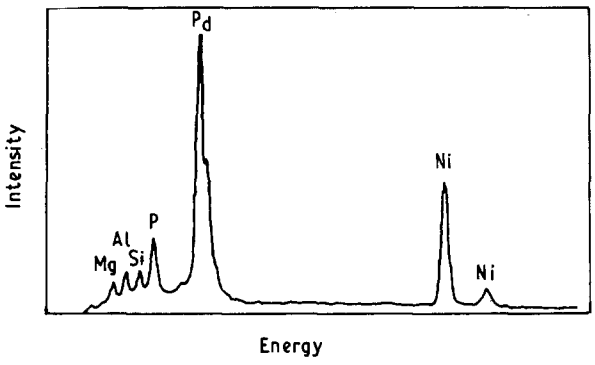

Figure 8 Electron probe X-ray energy spectrum at the centre of the dendrites with sample T_i of 1050 K.

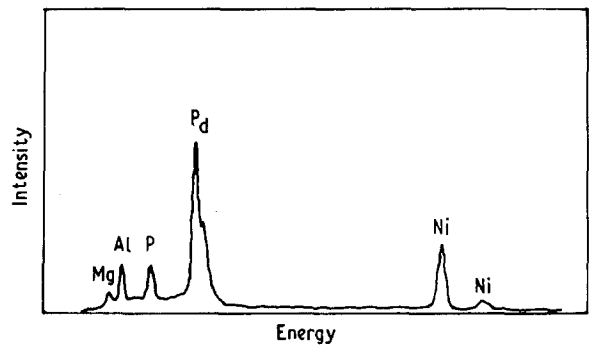

Figure 9 X-ray energy spectrum at the centre of the dendrites with sample T_i of 1250 K.

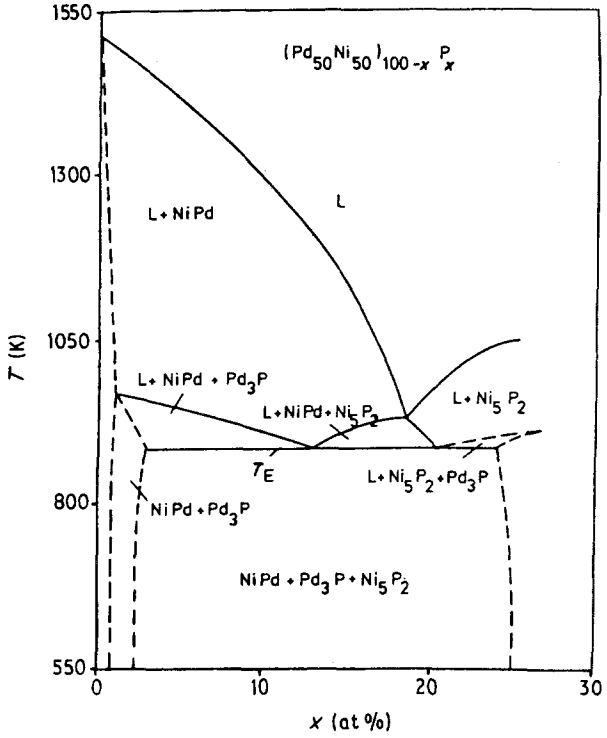

Figure 10 Section of the phase diagram of the ternary Pd–Ni–P alloy.

of the T_i on the morphology of the $Pd_{40}Ni_{40}P_{20}$ droplets can be interpreted.

To know what phase is initially formed, it is necessary to understand the phase composition in the $Pd_{40}Ni_{40}P_{20}$ alloy. The structure of the ternary Pd–Ni–P system in the composition range $(Pd_{50}Ni_{50})_{100-x}P_x$ with $0 < x < 25$ has been investigated by Wachtal *et al.* [9], who reported that $Pd_{40}Ni_{40}P_{20}$ alloy is composed eutectically by a Pd–Ni solid solution phase, and primary phosphide Ni_5P_2 and Pd_3P phases (see Fig. 10). As the $Pd_{40}Ni_{40}P_{20}$ melt cooled from above liquidus, the phosphide Ni_5P_2 phase would initially form. Donovan *et al.* have examined the structure of these phases in a slowly cooled $Pd_{40}Ni_{40}P_{20}$ alloy by transmission electron microscopy [10]. They identified the composition primary phosphide as $Pd_{34}Ni_{45}P_{21}$, the other two phases being $Pd_{40}Ni_{59}P_1$ and $Pd_{68}Ni_{14}P_{18}$ (absolute error is ± 10 at %). In the Pd–Ni solid solution phase the P content is almost absent, the third phase is a Pd-rich phosphide. Considering the error introduced by the energy spectrometer, the Ni-rich phase $Pd_{34}Ni_{45}P_{21}$ is very close to our primary phase $Pd_{36.2}Ni_{51.4}P_{12.4}$. Now, we can conclude that with the cooling rate decreased, the Ni-rich phase is initially formed on the heterogeneities; then the dendrites grow; and finally the lamellae structures eutectically grow on the dendrites radially.

6. Conclusions

Drop tube processing allows significant levels of liquid undercooling by elimination of crucible-induced nucleation. By controlling the processing parameters such as drop size, initial temperature and gas pressure, the solidification morphology of $Pd_{40}Ni_{40}P_{20}$ drops

from glass to crystal nucleation and growth was observed. As the cooling rate decreased, the Ni-rich phase $Pd_{36.2}Ni_{51.4}P_{12.4}$ was initially formed, and on this phase the dendrites grew into a glass matrix, then the surrounding eutectic crystals grew radially. As the initial temperature of melt increased, the heterogeneities were partly dissolved or reduced. From the experiment the density of nuclei was estimated as $1.4 \times 10^{13}/m^3$. The calculation of the cooling behaviour of drops in inert gas indicated that a cooling rate of 150 K/s is required for glass formation in drop tube processing.

References

1. A. J. DREHMAN and D. TURNBULL, *Scripta Metall.* **15** (1981) 543.
2. J. STEINBERG, A. E. LORD, Jr., L. L. LACY and J. JOHNSON, *Appl. Phys. Lett.* **38** (1981) 135.
3. D. S. SHONG, J. A. GRAVES, Y. UJIIE and J. H. PEREPEZKO, in "Materials processing in the reduced gravity environment of space", edited by R. H. Doremus and P. C. Nordine (Materials Research Society, Pittsburgh, Pennsylvania, 1987) p. 17.
4. A. J. DREHMAN and A. L. GREER, *Acta Metall.* **32** (1984) 323.
5. J. K. McCOY, A. J. MARKWORTH and R. S. BRODKEY, in "Materials processing in the reduced gravity environment of space", edited by R. H. Doremus and P. C. Nordine (Materials Research Society, Pittsburgh, Pennsylvania, 1987) p. 164.
6. R. A. SVEHLA, in "Estimated viscosities and thermal conductivities of gases at high temperature", Table 3 (NASA Technical Report R-132, 1962) p. 114.
7. H. A. DAVIES, in "Rapidly quenched metals III", Vol. 1, edited by B. Cantor (The Metals Society, London, 1978) p. 1.
8. A. J. DREHMAN, A. L. GREER and D. TURNBULL, *Appl. Phys. Lett.* **41** (1982) 716.
9. E. WACHTEL, H. HAGGAG, T. GODECKE and B. PREDEL, *Z. Metallkde* **76** (1985) 120.
10. P. E. DONOVAN, P. V. EVANS and A. L. GREER, *J. Mater. Sci. Lett.* **5** (1986) 951.

Received 10 August 1989
and accepted 6 June 1990